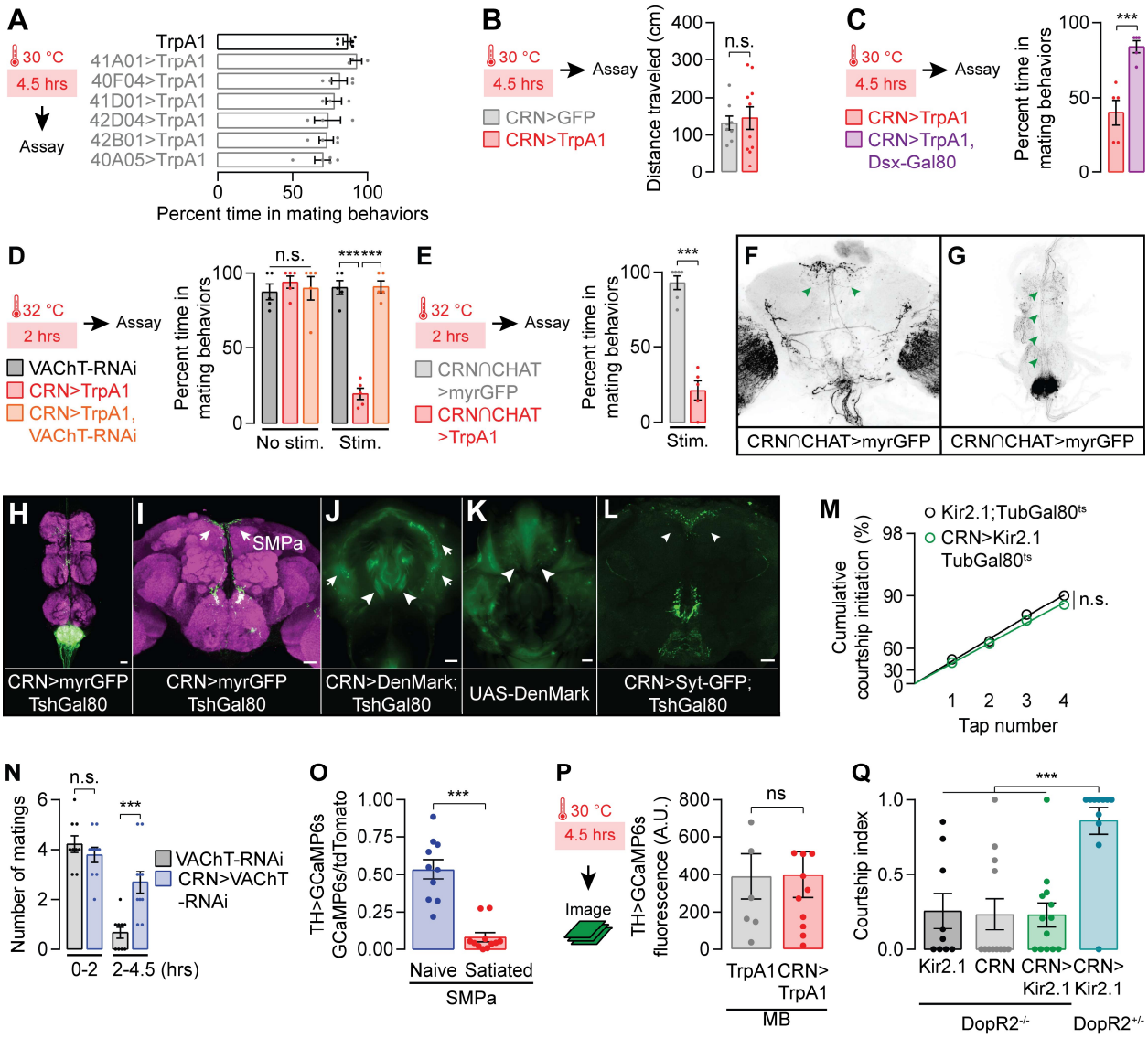

Figure S1. Cholinergic Copulation Reporting Neurons promote satiety in response to mating. Related to Figure 1. (**A**) Thermogenetic pre-stimulation of the non-CRN Gal4 lines derived from the Dsx locus does not induce satiety (n = 3-5 groups of 5-7 males; scored 30 minutes into the satiety assay). (**B**) Thermogenetic pre-stimulation of neurons labeled by R42G02-Gal4 (the CRNs) does not change the males' subsequent locomotor activity in a 10-min assay (n.s. not significant, t-test, n = 8-10 males). (**C**) A Gal80 transgene indirectly controlled by the Dsx locus (Dsx-LexA>LexAop-Gal80) blocks the decreased motivation seen following CRN stimulation (***p<0.001, t-test, n = 5 groups of 5-7 males each). (**D**) RNAi knockdown of VAChT prevents CRN stimulation from inducing satiety (n.s. not significant, ***p<0.001, one-way ANOVA, n = 5 groups of 5-7 males each). (**E-G**) Thermogenetic stimulation of the population co-labeled by CHAT-DBD and 42G02-p65AD (images in F-G) induces satiety (E) (***p<0.001, t-test, n = 5-6 groups of 5-7 males). Green arrowheads point to the ascending projections seen in Figures 1F and 1H. (**H-J**) R42G02-Gal4 with TshGal80 labels abdominal ganglion neurons (H) that project dendrites to external genitalia (J) and send axons to the top of the brain (I). In I, arrows point to the SMPa. In J, arrows point to dendritic terminals. (**K**) No labeling of the male's external genitalia in the no-Gal4 control for Figure 1G (scale bar = 20 μm). Arrowheads point to the male genitalia. (**L**) The ascending projections of CRNs are positive for GFP-tagged Synaptotagmin 1, which

labels axons (scale bar = 20 μm). Arrowheads point to the SMP. (**M**) Silencing the CRNs does not change the tap-induced courtship probability (a readout of mating drive) in males that have never mated (n.s. not significant, bootstrap, n = 30-31 males). (**N**) RNAi knockdown of VAChT in the CRNs increases the number of matings in a satiety assay (n.s. not significant, ***p<0.001, one-way ANOVA, n = 9-10 males). (**O**) Satiety decreases GCaMP6s fluorescence of dopaminergic projections to the SMPa (***p<0.001, t-test, n = 10-11 male brains). (**P**) Thermogenetic stimulation of the CRNs does not change the GCaMP6s fluorescence of dopaminergic projections to the mushroom body (MB) (n.s. not significant, one-way ANOVA together with Figure 1K, n = 30-31 males). (**Q**) Silencing the CRNs does not rescue the low courtship exhibited by DopR2 mutants that cannot receive the motivating dopamine signal (***p<0.001, one-way ANOVA, n = 9-13 males). For all figures, see Table S1 for the exact numbers of animals and experimental conditions used in each experiment.

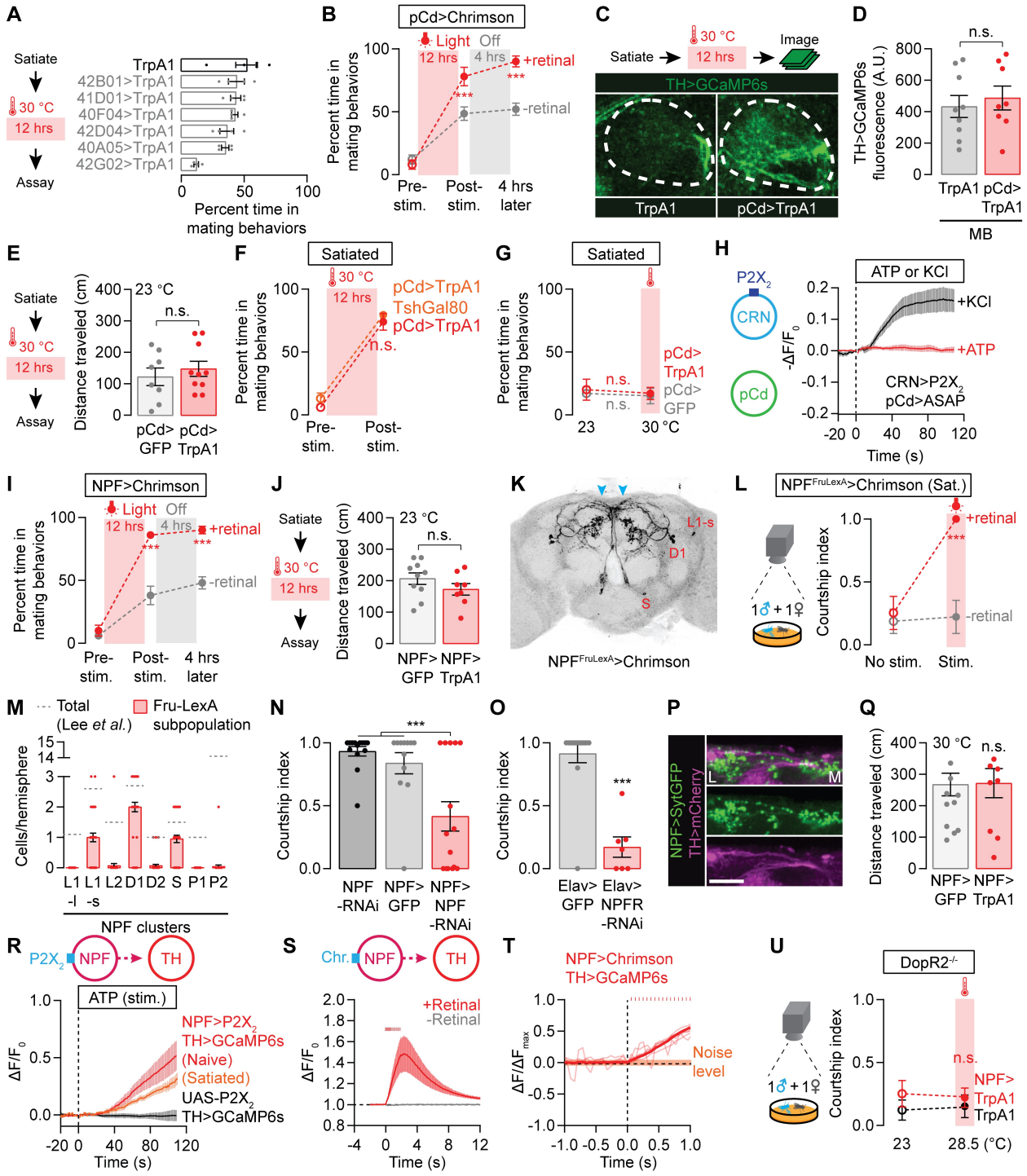

Figure S2. Neuronal control of motivational recovery. Related to Figure 2. (**A**) Thermogenetic stimulation of non-pCd Gal4 lines derived from the Dsx locus does not accelerate the recovery from satiety (n = 4-5 groups of 5-7 males). Stimulating the satiety-inducing CRNs (R42G02-Gal4) slows the recovery from satiety, as expected from the results in Figure 1. (**B**) 12-hr optogenetic stimulation of pCd neurons accelerates the recovery from satiety, an effect that lasts long after the stimulation ceases (***p<0.001, two-way ANOVA, n = 5 groups of 5-7 males each). (**C**) Thermogenetic, post-satiety stimulation of pCd neurons accelerates the recovery of calcium activity in dopaminergic projections to the SMPa. See Figure 2C for quantification. (**D**)

Thermogenetic, post-satiety stimulation of pCd neurons does not change the GCaMP6s fluorescence of dopaminergic projections to the mushroom body (MB) (n.s. not significant, one-way ANOVA together with Figure 2C, n = 10-11 male brains). (**E**) Thermogenetic, post-satiety stimulation of pCd neurons does not change subsequent locomotor activity in a 10-min assay (n.s. not significant, t-test, n = 8-10 males). (**F**) TshGal80 does not prevent pCd stimulation from recharging mating drive (n.s. not significant, two-way ANOVA, n = 5 groups of 5-7 males each). (**G**) Acute pCd stimulation does not revert satiety (two-way ANOVA, 5 groups each). (**H**) $P2X_2$ stimulation (+ATP) of the CRNs evokes no immediate change in the membrane potential of pCd neurons; KCl addition serves as a positive control for monitoring membrane dynamics (n = 7-8 male brains). (**I**) 12-hr optogenetic stimulation of NPF neurons accelerates the recovery from satiety, an effect that lasts long after the stimulation ceases (***p<0.001, two-way ANOVA, n = 5 groups of 5-7 males each). (**J**) Thermogenetic, post-satiety stimulation of NPF neurons does not change subsequent locomotor activity (n.s. not significant, t-test, n = 8-10 males). (**K-L**) CsChrimson-mediated [S1] acute optogenetic activation of Fru^+ NPF neurons (K), which also project to the SMPa (arrowheads), immediately reverts satiety (L) (two-way ANOVA, n = 9-14 males). (**M**) Fru-LexA labels ~4 NPF neurons. Dashed lines indicate the total population of NPF neurons based on a previous report [S2] (n = 42 hemispheres). (**N-O**) Knockdown of NPF in NPF neurons (N), or NPFR in all neurons (O), decreases courtship (one-way ANOVA, N: n = 12-15 males, O: n = 7-14). (**P**) NPF neurons' axons (green) and dopamine neurons' processes (magenta) are intermingled at the SMPa. Letters L and M delineate the medial-lateral axis. The scale bar represents 20 μm. (**Q**) Acute thermogenetic, post-satiety stimulation of NPF neurons does not change the locomotor activity of the males during 10 minutes of stimulation (n.s. not significant, t-test, n = 10-14 males). (**R**) $P2X_2$ stimulation of NPF neurons evokes a strong calcium transient (measured with GCaMP6s) in dopaminergic neurons. The excitation is moderately reduced in brains of satiated males. (n = 7-8 male heads). (**S-T**) Optogenetic stimulation (8 ms pulses, 15.5 Hz for 2 s) of NPF neurons with CsChrimson induces a strong calcium transient (measured with GCaMP6s) in dopaminergic neurons (n = 5-7 male heads) (S). The calcium transients start in the frame of the first light pulse (red tick) (n = 7 male heads) (T). Since each frame takes ~64 ms to scan and the pulses take place during the first 8 ms of each frame, the delay time can at most be 56 ms (see STAR Methods). The orange shading in (T) indicates the 95% confidence interval of the fluorescence fluctuation before stimulation (an estimate of the noise level). (**U**) Thermogenetic stimulation of NPF neurons does not overcome the reduction in courtship seen in males lacking DopR2 (two-way ANOVA, n = 12-15 males).

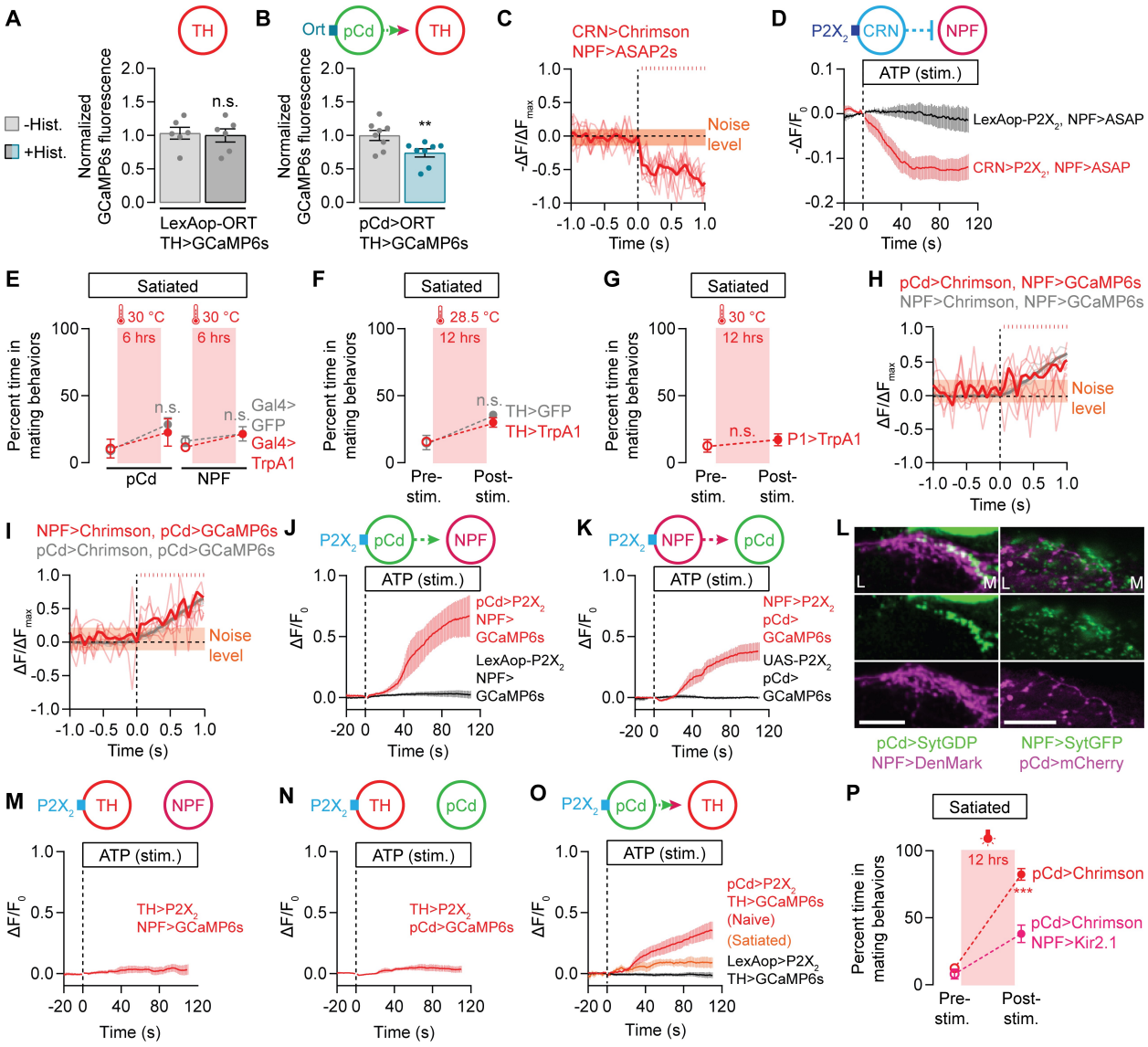

Figure S3. Recurrent activity between pCd and NPF (but not dopaminergic) neurons. Related to Figures 2 and 3. (**A-B**) Chemogenetic silencing of pCd (B) neurons reduces baseline calcium activity in dopaminergic projections to the SMPa (***p<0.001, **p<0.01, n.s. not significant, one-way ANOVA together with Figure 2M, A: n = 6 male brains, B: n = 8). See Figure 2M for similar experiments that silence NPF neurons. (**C**) Acute optogenetic stimulation (8 ms pulses, 15.5 Hz for 2 s) of the CRNs triggers a rapid hyperpolarization in the NPF neurons with a delay equal to or less than 56 ms (see STAR Methods) (n = 8 male brains; red traces use the same data set as in Figure 2O, here normalized to ΔF_{max} for each trial). Orange shading indicates the 95% confidence interval of the fluorescence fluctuation before stimulation (an estimate of the noise level). (**D**) Acute $P2X_2$ stimulation of the CRNs decreases the membrane potential of the NPF neurons (n = 7 male brains each). (**E**) Thermogenetic, post-satiety stimulation of either pCd or NPF neurons for 6 hours does not accelerate the recovery from satiety (n.s. not significant, two-way ANOVA, n = 4-5 groups of 5-7 males). (**F-G**) Thermogenetic stimulation of either dopaminergic (F) or P1 (G) neurons does not recharge mating drive after satiety (n.s. not significant, two-way ANOVA, F: n = 4 groups of 5-7 males each, G: n = 6 groups). (**H-I**) Acute optogenetic stimulation (8 ms pulses, 15.5 Hz for 2 s) of either pCd (H) or NPF (I) loop neurons

elicits a rapid calcium transient in the other population with a delay equal to or less than 120 ms (H) and 56 ms (I), respectively (see STAR Methods) (H: n = 5-6 male brains, I: n = 5-6; red traces in the two panels use the same data sets as in Figures 3C and 3D, here normalized to ΔF_{max} for each trial). Orange shading indicates the 95% confidence interval of the fluorescence fluctuation in the red traces before stimulation (an estimate of the noise level). (**J-K**) Acute $P2X_2$ stimulation of either pCd (J) or NPF (K) neurons induces strong calcium transients in each other (J: n = 8 male brains each, K: n = 6-7). (**L**) Left: pCd neurons' axons (green) and NPF neurons' dendrites (magenta) are intermingled at the SMPa. Right: NPF neurons' axons (green) and pCd neurons' processes (magenta) are intermingled at the SMPa. Letters L and M delineate the medial-lateral axis. The scale bar represents 20 μm. (**M-N**) Chemogenetic activation of dopaminergic neurons does not evoke strong calcium transients in either NPF (M) or pCd neurons (N) (M: n = 8 male brains, N: n = 7). (**O**) $P2X_2$ stimulation of pCd neurons evokes a calcium transient in dopaminergic neurons. The excitation is significantly reduced in brains of satiated males. (n = 7-8 male heads). (**P**) Silencing NPF neurons with the potassium channel Kir2.1 prevents pCd stimulation from recharging mating drive (***p<0.001, two-way ANOVA, n = 5 groups of 5-7 males each).

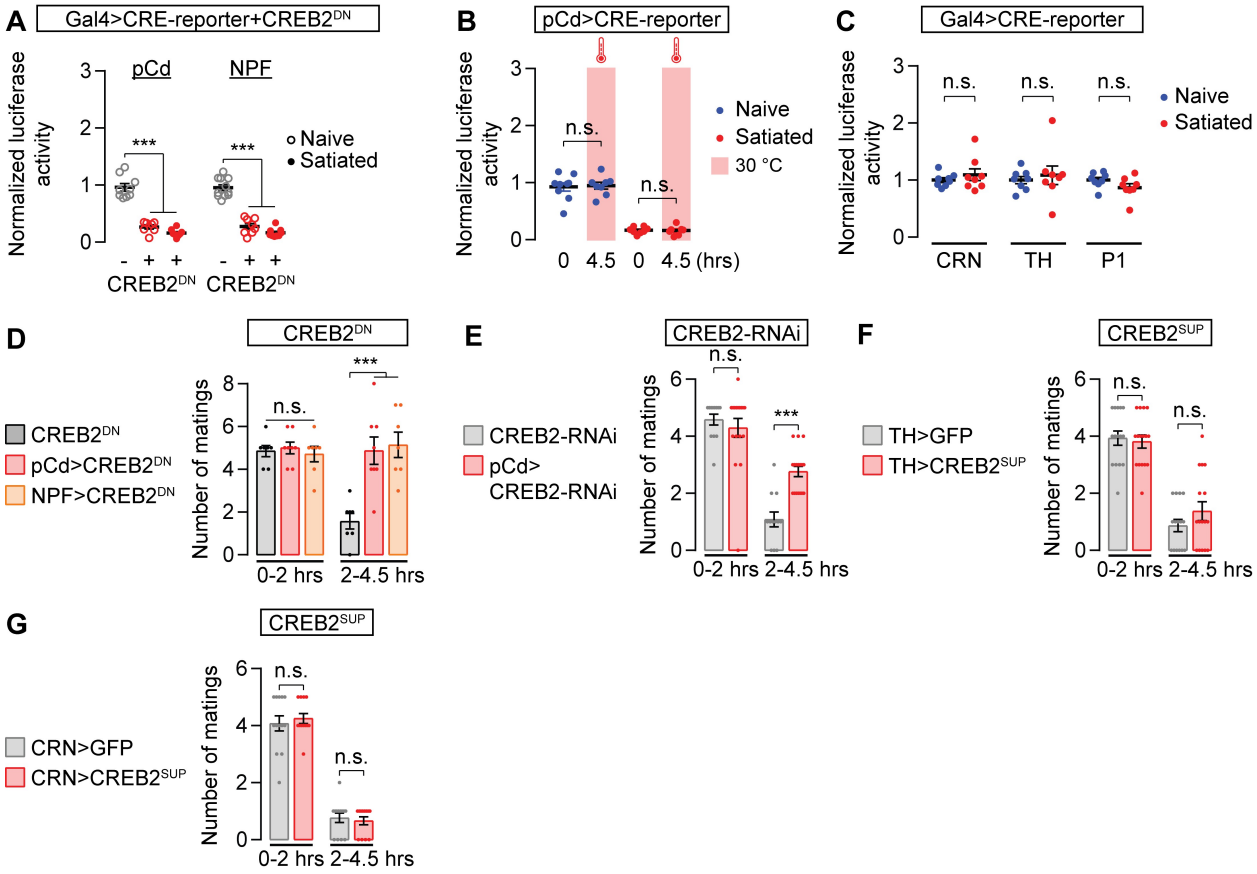

Figure S4. CREB2 in motivational circuitry. Related to Figure 4. (**A**) Expressing dominant-negative CREB2 [S3] in either pCd or NPF neurons decreases CREB2 activity in these neurons to a satiety-like level (***p<0.001, one-way ANOVA, n = 7-11 groups of 3 male brains). (**B**) Elevated temperature alone does not change CREB2 activity in pCd neurons (n.s. not significant, one-way ANOVA, n = 7-9 groups of 3 male brains). (**C**) CREB2 activity does not change with satiety in either the CRNs, dopaminergic neurons, or P1 neurons (n.s. not significant, one-way ANOVA, n = 8 groups 3 male brains each). (**D-E**) Expressing either dominant-negative CREB2 (D) or an RNAi construct targeting CREB2 (E) in pCd neurons increases the number of matings in the satiety assay (***p<0.001, n.s. not significant, one-way ANOVA, D: 7-8 males, E: n = 12-17 males). (**F-G**) Expressing the transcription suppressing isoform of CREB2 in dopaminergic neurons or CRNs does not alter mating drive (n.s. not significant, one-way ANOVA, F: n = 15-16 males, G: n = 12-13).

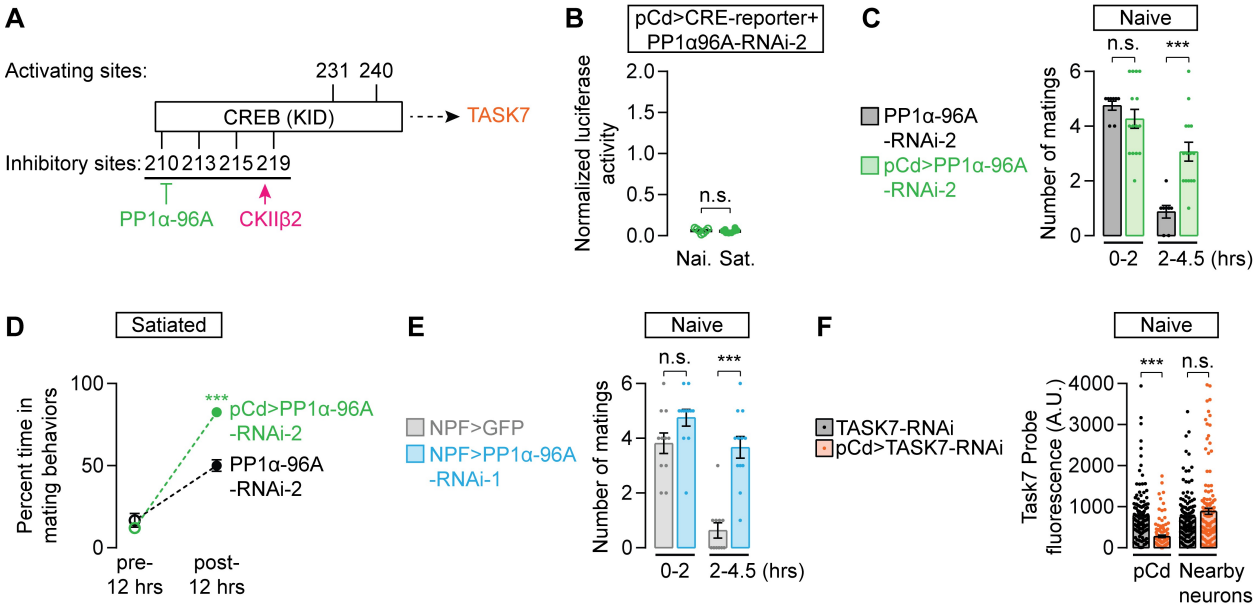

Figure S5. Molecular machinery controlling CREB2 activity in recurrent circuitry. Relate to Figure 5. (**A**) Model of CREB2 regulators and transcription targets. (**B-D**) Knocking down PP1α96A using a second, independent RNAi from that in Figures 5A-5C decreases CREB2 activity (B), increases mating drive (C), and speeds the recovery from satiety (D) (***p<0.001, n.s. not significant, B: one-way ANOVA with Figure 5A, C: one-way ANOVA, D: two-way ANOVA; B: n = 7-8 groups of 3 male brains, C: n = 8-15 males, F: n = 5-6 groups of 5-7 males each). (**E**) Knocking down PP1α96A in NPF neurons also increases mating drive (***p<0.001, n.s. not significant, one-way ANOVA, n = 11-12 males). (**F**) RNAi knockdown of Task7 in the pCd neurons decreases their transcript level of Task7, demonstrating the effectiveness of the UAS-RNAi construct and the smFISH probes (***p<0.001, n.s. not significant, one-way ANOVA, n = 122-145 cells in 14-17 male brains).

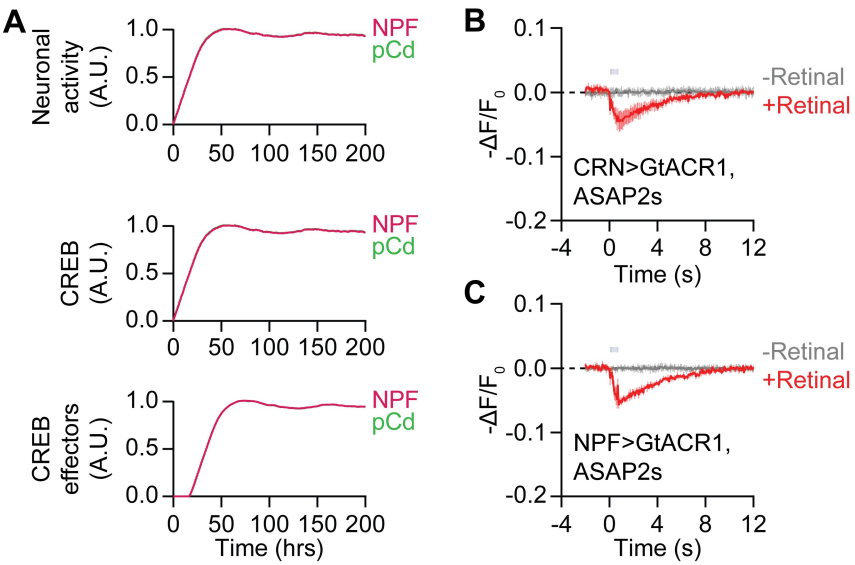

Figure S6. The mating-drive model. Related to Figures 6 and 7. (**A**) Neuronal activity, CREB2 activity, and CREB2 effector levels equilibrate to a steady state in both pCd and NPF neurons. The green pCd line is largely obscured behind the magenta NPF line (**B-C**) Optogenetic silencing (5 ms pulses, 10Hz for 0.67 s) of either the CRNs (B) or the NPF neurons (C) hyperpolarizes their membrane potentials, as measured by the voltage sensor ASAP2s (B: n = 5-6 male brains, C: n = 5 each).

Figure (first occurrence)	Result	Evidence in data from [S4] (31,138 cells)	Evidence in data [S5] (56,902 cells)
2I	NPFR expression in dopamine neurons	NPFR detected in 3/290 dopamine neurons (elav+ nsyb+ ple+)	NPFR detected in 40/651 dopamine neurons (elav+ nsyb+ ple+)
4B	CREB2 expression in pCd neurons	CREB2 detected in 11/47 putative pCd neurons (elav+ nsyb+ dsx+ fru-)**	CREB2 detected in 8/67 putative pCd neurons (elav+ nsyb+ dsx+ fru-)**
4C	CREB2 expression in NPF neurons	CREB2 detected in 29/163 npf neurons (elav+ nsyb+ npf+)	CREB2 detected in 48/541 npf neurons (elav+ nsyb+ npf+)
5A	CKIIβ2 expression in pCd neurons	N/A***	N/A***
5A	PP1α96A expression in pCd neurons	PP1α96A detected in 15/47 putative pCd neurons (elav+ nsyb+ dsx+ fru-)**	PP1α96A detected in 42/67 putative pCd neurons (elav+ nsyb+ dsx+ fru-)**
		PP1α96A detected in 6/11 CREB2+ putative pCd neurons (elav+ nsyb+ dsx+ fru- CREB2+)**	PP1α96A detected in 5/8 CREB2+ putative pCd neurons (elav+ nsyb+ dsx+ fru- CREB2+)**
5H	Task7 expression in pCd neurons	Task7 detected in 8/47 putative pCd neurons (elav+ nsyb+ dsx+ fru-)**	Task7 detected in 28/67 putative pCd neurons (elav+ nsyb+ dsx+ fru-)**
		Task7 detected in 2/11 CREB2+ putative pCd neurons (elav+ nsyb+ dsx+ fru- CREB2+)**	Task7 detected in 6/8 CREB2+ putative pCd neurons (elav+ nsyb+ dsx+ fru- CREB2+)**
S5E	PP1α96A expression in NPF neurons	PP1α96A detected in 75/163 NPF neurons (elav+ nsyb+ npf+)	PP1α96A detected in 340/541 NPF neurons (elav+ nsyb+ npf+)
		PP1α96A detected in 20/29 CREB2+ putative pCd neurons (elav+ nsyb+ npf+ CREB2+)	PP1α96A detected in 30/48 CREB2+ putative pCd neurons (elav+ nsyb+ npf+ CREB2+)

Table S2. Supporting evidence from reanalyses of single-cell sequencing datasets. Related to Figures 2, 3 and 5.

*We used data from wild-type flies of all ages. **This labeling strategy also includes some pC1/pC2 neurons and excludes the 1-2 fru+ pCd neuron per brain. ***CKIIβ2 was not detected across the entire dataset

Index	Task7 Probes	Dsx Probes
1	aagggtacggacattctgtc	attccagttctcctccgaaa
2	gtgaaagtgcataccaccag	atcatgtccgagtcggacat
3	ggcggctccaattaaaagat	cacagacgtcgttctttgag
4	gtgactccagggaatcgaac	aaatcgagctgccgctggaa
5	taggaattcccatcttttgg	ctttagggtgatctttaggc
6	caaagttgttcttaacggtc	aacttgcagtaccgcttgtg
7	tcgtcagtcacattgtactt	acttctcgcacgtgcagtag
8	acgatttccatcacacggaa	ctgcgacatgatggtgatga
9	cttgtggggcttattttcaa	atggtgggcgtggacatgag
10	gaaagctccagcgaatttcc	acatgtccgtgatgcgagtg
11	ccagtacaaccgtgctgaaa	gtgaccgtggatgctggaag
12	gcgtagaatgaccatatcct	attgctggaactgggtgctc
13	gcttttcccggaattgtaac	gctagtgatcaccgatgttc
14	catagcatagcccatacaaa	cggaagtggacgacggcgag
15	agactggaacatcaccagac	gagatcggcaaaatggctgc
16	acttattcagacgttctccg	cgttctttcgattgacggaa
17	cgccttattatcacggatgc	aaaacgtcttggcccaaggg
18	atgagattcatttcggtggc	tagcttttggcaatagtcta
19	attatggaggagagcattcc	aaggatagcggaatttttct
20	cctcgtatcgggaaaagact	tacatgagtggcatcagctc
21	gaagctatcgaagtagctcc	gtctgcgtcctttaatatca
22	gtcgtcaaggtgacaaaaca	gggaagcctcttcaatgttg
23	cacataatcgccgaaaccaa	tttatttccactcgagcctc
24	gagcttggtcgttctgcaat	gtagatctgggctacagtgc
25	cacatagccaggcttattag	ccatcggggtgtagtagttg
26	agccgaataggatgaagacc	cgggtaggtcaggtacatgg
27	aatagattgatactggcggc	catagcgaccctgttcgatg
28	ttgcatggtcatgaatcgga	tgagcggcagatgggtgaag
29	tgctcatctctcttggcatc	ggagtcggtggacaaatctg
30	atttccagccaagttctgag	gagggcttttggttgtggac
31	gactcatcatcgaaggtcac	tggtgaccattgtgggtgag
32	cttgccgtgcatattgtacg	aacgttgcgatactgctacg
33	gttgtgtagttgttctccag	tatcgacgaagaggacagcg
34	atgcaggtgcaggaacacag	
35	cgaactgctcatgattcagg	
36	atgtcggtaggctgaaagtc	
37	ttcaggcacaaggtgctctc	

Table S3. smFISH probes for Task7 and Dsx. Related to Figure 5.

SUPPLEMENTAL REFERENCES

S1. Klapoetke, N.C., Murata, Y., Kim, S.S., Pulver, S.R., Birdsey-Benson, A., Cho, Y.K., Morimoto, T.K., Chuong, A.S., Carpenter, E.J., Tian, Z., *et al.* (2014). Independent optical excitation of distinct neural populations. Nat. Methods *11*, 338–346.

S2. Lee, G., Bahn, J.H., and Park, J.H. (2006). Sex- and clock-controlled expression of the neuropeptide F gene in Drosophila. Proc. Natl. Acad. Sci. U. S. A. *103*, 12580–12585.

S3. Eresh, S., Riese, J., Jackson, D.B., Bohmann, D., and Bienz, M. (1997). A CREB-binding site as a target for decapentaplegic signalling during Drosophila endoderm induction. EMBO J. *16*, 2014–2022.

S4. Croset, V., Treiber, C.D., and Waddell, S. (2018). Cellular diversity in the Drosophila midbrain revealed by single-cell transcriptomics. Elife *7*, e34550.

S5. Davie, K., Janssens, J., Koldere, D., Waegeneer, M. De, Pech, U., Kreft, Ł., Aibar, S., Makhzami, S., Christiaens, V., González-Blas, C.B., *et al.* (2018). A Single-Cell Transcriptome Atlas of the Aging Drosophila Brain. Cell *174*, 1–17.